Discrete Fiber Optic Sensing Techniques for Structural Health Monitoring of Bridges

Farhad Ansari

Synopsis: From the very beginnings of time mankind has been intrigued with the potential applications of light and the possibilities that it could bring about. The origins of optical fibers probably go back to mid 19th century when the scientists tried to guide, bend, and transmit the light from one location to another. Now, optical fibers have found widespread usage in telecommunications as well as in medical and sensing applications. This article provides a summary review of principles involved in sensing with discrete optical fibers such as Bragg gratings and specific methods more prevalently employed in monitoring of bridges. The focus will be in application examples including monitoring of the masonry vaults of the Brooklyn Bridge, deformation of cable stays, and fiber optic accelerometers for testing of bridges.

Keywords: Cracks; Damage; Fiber Optic Sensors; Structural Health Monitoring; FBG; Bridges; Stay Cables; Brooklyn Bridge;

Farhad Ansari is Professor and Head of the Civil and Materials Engineering Department at the University of Illinois in Chicago. His area of research is in fiber optic sensors and structural health monitoring of bridges. He is currently the president of ISHMII which is an international society for health monitoring of civil structures.

INTRODUCTION

Structures are monitored because of safety concerns, diagnostics and problem solving, forensic analysis, and condition assessment. In addition to routine visual assessments, survey of literature reveals the existence of many approaches for monitoring of structures including strain and deformation based techniques, vibration analysis, acoustics, and optical techniques. The practice of structural health monitoring (SHM) in mechanical and aeronautical systems has advanced to the stage where they now involve step-by-step text book procedures. However, the same is not true for civil structures and in particular for bridges. In comparison to mechanical systems, bridges are rather large and massive; exposed to ambient and environmental conditions; composed of several types of materials some inherently heterogeneous; possess many connections, splices, and expansion joints and less than ideal boundary conditions, manufactured while exposed to external elements, and under traffic or operation at the time of monitoring. Therefore, an effective strategy for monitoring of bridges requires a sound strategy for engineering analysis of the structural problems, economical placement of sensors and sensor types, interpretation of sensor data, quantitative analysis of the structure and correlation of the bridge issues with SHM results.

An important element in structural health monitoring is selection and placement of sensors suitable for measurement of key parameters that influence the performance, service requirements, and health of the structural system. In many recent applications, optical fiber sensors have emerged as sensors of choice. This is due to the fact that fiber optic sensors possess many attributes of interest in civil structural monitoring, including: single channel distributed sensing, geometric adaptability, immunity to electrical and magnetic interference, elimination of lead lines, optical transfer of information, high resolution, and high signal to noise ratio. Optical fibers transduce physical or ambient perturbations through intensity modulation, wavelength shifts, frequency changes, and interference of the optical signals. A number of sensor types have been developed based on these principles including Fiber Bragg Gratings (FBG), Fabry Perot (FP) and long gauge white light sensors (Ansari, 2007). However, other sensor designs such as those based on intensity modulations of light waves as well as Brillouin scattering distributed sensors have been developed and effectively employed in civil engineering applications (Glisic, et al, 2010, 2011, Gu, et al, 2000, Wu et al, 2010, Bao et al., 2002, Yuan, et al , 1997, Zhao et al, 2002). Over the years, FBG sensors have transcended from laboratory bench tops to full scale mass production for applications in bridges, tunnels, dams, high rise buildings and other types of structures. One of the practical advantages of FBG sensors is the capability for serial multiplexing of several sensors along a single optical fiber cable. This feature reduces both the number of lead cables necessary for transmission of the sensor signals as well the number of data acquisition channels in the optical interrogation instrument. These features render the sensor practical and cost effective for structural monitoring. This article focuses on some of the applications of FBG sensors in monitoring of bridges. Applications in three different bridges and measurement types are presented.

FIBER BRAGG GRATING SENSORS

The transduction mechanism in FBG sensors is based on the modulation of the wavelength of the optical signal travelling through the fiber. In essence, Bragg Gratings are produced by physical exposure of the optical fiber core to intense radiation of a UV laser. A mask is used to create a periodic change in the pitch of the grating in the optical fiber core. The pitch of the grating signifies the wavelength sensitivity of the grating. Bragg Gratings are typically 10 mm or so in length and the grating pitch can be selected to reflect specific wavelength components of the optical signal. Strain induced changes to the pitch of the FBG sensors result in proportionate variation in the wavelength of the signal (Fig. 1). The modulated light wave is then transmitted to an interrogation system for detection and demodulation. Calibration is required to convert the optical change into the measurand of interest, i.e. strain. In a manner similar to strain gages, calibration of optical fibers is related to the strain and temperature sensitivities of the fiber by appropriate gage factors. A complete review of theoretical basis for the establishment of strain and temperature sensitivities is given by Measures (2001). A brief description is given here for completeness.

The opto-thermo-mechanical process involved in fiber optic sensing relies on the optical path length, L_n, which is the product of the gauge length, L, and the core refractive index, n:

$$L_n = Ln \tag{1}$$

While L corresponds to the gauge length of the interferometric sensor, for FBG, L corresponds to the period of the Bragg and not the length of grating. FBG is sensitive to both changes in strain, $\Delta\varepsilon$ and in temperature ΔT. In the case of uniaxial strain field and the absence of thermal gradients, the strain is related to the change in the optical path length by way of the gauge factor, G_ε:

$$\frac{\Delta L_n}{L_n} = G_\varepsilon \Delta\varepsilon \tag{2}$$

In Eq. (2)The change in optical path length is proportional to the wavelength change:

$$\frac{\Delta L_n}{L_n} = \frac{\Delta\lambda}{\lambda} \tag{3}$$

Where, λ and $\Delta\lambda$ are the Bragg wavelength, and the wavelength shift in FBG, respectively. Therefore, the gage factors for FBG sensor is defined as:

$$G_F = \frac{\Delta\lambda / \lambda}{\varepsilon} \tag{4}$$

Eq. (4) is similar to the relationships for resistance strain gauges where the gauge factor, G_R defines the calibration factor relating the resistance change, $\Delta R/R$ to the strain, ε:

$$G_R = \frac{\Delta R / R}{\varepsilon} \tag{5}$$

The calibration process for any of the FBG sensor is accomplished by mounting of the sensor to a calibration beam which is deflected to produce a known strain ε. The wavelength change is measured and the corresponding gauge factor is determined by Eq. (4).

APPLICATIONS

The Brooklyn Bridge

The Brooklyn Bridge approach structure on the Manhattan side of the East River was constructed over a series of increasingly taller and longer brick masonry vaults. The vaults that are the subject matter of this investigation are the two largest spans of the approach structure with span lengths of 10 and 10.4 m (32.8 and 34.1 ft), respectively. Longitudinal crown cracks covering the entire lengths of these cylindrical vaults were discovered during a routine inspection in 1996. The double-span vaults are seated on the walls of two 3-story masonry buildings. The structure to the west of these vaults is a steel truss and on the east is the bridge abutment as shown in Fig. 2. The bridge abutment is a masonry counterweight constructed on top of the steel anchorage for the main bridge cables. Visual inspection of the three floor levels and the basements in both structures also revealed existence of a vertical crack through the adjoining wall supporting the vaults. This crack was approximately halfway between the north and south ends of the structure, and ran from the seat of the vaults on third floor all the way to the exposed portion of the foundation in the basement (Fig. 3). In addition, other vertical cracks were present on the adjoining support wall as well as the support wall for the west vault, but they were confined to the upper levels of the structure. Details regarding the instrumentation and SHM of the vaults are given elsewhere (Talebinejad, et al., 2011). Some of the SHM details are provided here.

Vaulted structures have been used throughout the centuries to support enormous structural loads. Because of the inherent geometric characteristics of the vaults, tensile stresses are eliminated and the loads are supported in compression. However, the vault thrust might push outward/inward as the bridge experiences overloading, foundation settlement or support displacement and thermal movements. As a result, cracks are formed in locations where line of thrust touches the boundaries of the vault (Fig. 4). The visual inspection observations were used in the decision making process in order to reduce the cost of the sensor installation and monitoring activities. In doing so, it was realized that the middle wall supporting the two vaults was considered most likely to have moved causing the vaults to crack. The cause for the formation of the main vertical crack in the middle wall could have been differential settlement of support following the construction of the bridge back in 1883, or excessive thrust from the vaults due to loads, and thermal gradients. The fact that the east wall was not cracked was attributed to confinement by the anchorage structure.

The sensor installation plan was based on the abovementioned considerations. The vault crown cracks were monitored by way of crack sensors, and to examine the movement of the walls, especially the middle vault, tiltmeters were used on all the floors. Temperature sensors were used on all the floor levels as well as at the vault locations in order to examine the effects of thermal gradients. Accelerometers were used for monitoring of traffic induced vibrations and the vibration of the wall in the basement adjacent to the anchorage. All the sensors were FBG based and a single optical interrogation unit was employed for the acquisition of sensor signals. Fig. 5 corresponds to the schematic front view of the vaults with sensor types and locations. Typical crack and tiltmeter sensors are shown in Fig.6. For detailed analysis of all the sensor data and considerations leading to the conclusions provided here reference should be made to Talebinejad, et al. (2011). A typical result is shown in Fig. 7 which corresponds to the correlation between the vault crack sensors and the temperature sensor signals from the west vault over a twelve months period. These results and the results from the east vault indicate that the mid section of the vault went through a crack opening displacement cycle with crack opening displacement as large as 1.2 mm (0.05 in), commensurate with thermal fluctuations. The west vault controls the movements, because the mid section of the vault expands and crack opening displacements increase for rise in temperature and contract for falling temperatures. In essence, the crown cracks were developed due to the movement of the middle wall and the confinement of the vaults by the anchorage and the truss structures.

Lingotto Cable Stayed Pedestrian Bridge

The Lingotto pedestrian bridge was constructed in Turin, Italy for the 2006 winter Olympic Games (Fig. 8). The bridge construction was completed in late 2005. The bridge was designed to link pedestrian traffic from the Olympic village to the Lingotto commercial center by spanning over railroad tracks separating the two. The bridge was designed with a complex geometry. For example, the bridge deck is constructed on a radius, has a vertical rise and fall slope, and the elliptical arch is set on a diagonal with cables at various levels. Due to the unusual design of the bridge, it was decided that sensors should be installed to monitor the structural health of the bridge. The objective of the monitoring was to record the cable displacements and vibrations to evaluate the condition of the bridge.

The main structural component of the bridge is a large parabolic arch. The cross section of the arch is triangular and constructed of 15 mm (0.59 in) thick plates. The triangular cross section had 3m sides at the base and rotates toward the top. The arch has a 55 m (180.4 ft) footprint and stands up to a height of 70 m (229.7 ft). The main bridge superstructure consisted of two edge beams, and additional framing spans between the two beams. The deck is reinforced concrete. The total length of the bridge is 368 m (1207.3 ft) and the main span is 150 m (492.1 ft). Eight pairs of cable stays support the main span of the bridge from the arch. There are eight pairs of cable stays on each side of the arch. The cables on opposing sides of the arch work together to anchor the arch and support the bridge span. The cables are spaced approximately 18.5 m (60.7 ft) along the span of the bridge. The cables consist of twisted steel wires. The steel cables consisted of three diameters; 55 mm (2.2 in), 60 mm (2.4 in), and 75mm (3 in).
The main sensors used for the structural health monitoring of the bridge consisted of specially designed Fiber Optic Bragg gratings (FBG). The FBG sensors were designed to measure dynamic deformations over a long gauge. Conventional sensors and accelerometers were also employed for monitoring of the deck. The fiber optic cable sensor used on the bridge is shown in Fig. 9. It includes a pre-tensioned FBG glued to angled supports at each end.

The FBG is protected by a PVDF (polyvinylidene difluoride**)** tube. After manufacturing, each sensor was installed on a cable to be tested and calibrated. During the calibration process, the sensor experiences several cyclic loads to assess repeatability, hysteresis, resolution and the sensitivity of the sensor. The induced changes in the wavelength of the sensor are calibrated against a high precision extensometer. The gauge factor for these sensors vary between 1.05 - 1.16. Fig. 10 shows a typical plot of the calibration test data. These sensors are capable of measuring strain and dynamic properties such as vibration frequency and damping ratios. The resolution of these sensors is typically rated at 1.2 με.

Twenty sensors were installed on the cables of the LingottoLingotto Bridge to continuously monitor the deformation and dynamic response of the cables. These sensors were installed on the cables near the end closest to the bridge deck. Fig. 11 shows a sensor mounted on one of the bridge cables. Data acquisition was accomplished by interrogator capable of acquiring the sensor data at a sampling frequency of 250 Hz and stored on an on-site computer.

In addition to monitoring the cable stays under ambient load conditions, static and dynamic load tests were conducted and the performance of the cables was recorded. Static load tests were completed by loading the bridge deck. Barrels were placed on the bridge deck and they were filled with water in sequence starting from the north side. Each of the 138 barrels was filled with 600 L (159 gallons) of water. After the tests, the barrels were emptied in the same manner. The strain in the FBG sensors was used to calculate the force in the cables and this was compared to the estimated design forces. Test setup for dynamic tests of the bridge included a 500 kg (1104 lb) concrete mass as a pendulum from a steel frame. The mass was hung at three different heights to excite the bridge at different natural frequencies. By swinging the pendulum mass, the bridge superstructure was excited. The pendulum setup was tested at three different locations along the span of the bridge.

Typical dynamic strain data as well as the frequencies computed from the cables are shown in Fig. 12 and 13. As shown in these figures the resolution of these types of sensors are extremely high and they were able to monitor the very low strain data from the measurements. The computer models found the first three natural frequencies of the bridge to be 0.454, 0.489, and 0.592 Hz. Because of the complex geometry of the bridge, almost all of the mode shapes are a combination of the lateral, bending and torsional deformations of the bridge. The first mode shape is lateral-torsional. In the second mode shape, the first bending mode shape is dominant. The third mode shape is the combination of lateral, bending and torsional deformation with more emphasis on the lateral movement.

Dynamic tests were done in both the longitudinal and transverse directions with different pendulum lengths. For the tests which were performed with pendulum oscillating in the transverse direction, nearly all of the sensors recorded a frequency of 0.54 Hz. Considering that the pendulum was swinging in the transverse direction, mode shapes which were dominated by the lateral deformation were more likely to be excited. So, it is evident that the third natural frequency of the bridge was captured with the fiber optic sensors.

Bridge Dynamics with Fiber Optic Accelerometers

Accelerometers are strategically placed in structures for the determination of dynamic characteristics and extraction of parameters such as natural frequencies and mode shapes. Typical sensing elements employed in the construction of accelerometers are piezoelectric and magnetostrictive materials. However, in recent years, fiber optic sensor accelerometers have become popular due to higher resolution and signal to noise ratios achieved in the applications. While the mass and spring systems form the basic structure of the accelerometers, various configurations have been employed for the construction of the fiber optic sensor accelerometers (Berkoff et al, 1996, Todd et al., 1998, Shi et al., 2003, Feng et al., 2011). A unique design was recently proposed by Talebinejad, et al (2009) where it utilizes a lumped mass and the stiffness of the optical fiber as the spring element. By employing this configuration, the FBG is always subject to uniform strain distribution along its length resulting in a sharp reflection with no broadening.

The simplest model of an accelerometer is a mass-spring system that is attached to an enclosing casing (Fig.14). The applied acceleration of the casing causes the mass to move, and this motion can be used to determine the magnitude of the acceleration. The equation of motion for the mass shown in Fig.4 is defined as:

$$m\ddot{x} + kx = -ma \tag{6}$$

Where, x is the displacement of the mass m relative to the casing, a is the ground acceleration and k is spring stiffness. Dividing both sides of the Eq.6 by the mass m and defining natural frequency of system by $\omega = \sqrt{k/m}$, result in:

$$\ddot{x} + \omega^2 x = -a \tag{7}$$

As shown in Fig.15, the design of the accelerometer involved stretching the optical fiber with FBG by a predetermined amount to achieve the required spring constant per accelerometer requirements. A lumped mass was attached to the fiber and guided through a precisely machined tube in order to eliminate the cross axis sensitivity. Modeling details and numerical simulation results for the evaluation of the sensor design are detailed in Talebinejad, et al (2009). The gauge factor was determined by the following relationship:

$$G = \frac{\Delta\lambda/\lambda}{a} \tag{8}$$

The calibration process was accomplished by mounting the FBG accelerometer along with a high-precision conventional piezoelectric accelerometer of known sensitivity on the cantilever beam. The wavelength shift due to the acceleration was measured during the experiments and employed in Eq.(8). Fig. 16 corresponds to a typical raw data from FBG accelerometer which is compared with the output of the conventional PZT accelerometer.

The accelerometers were also employed in testing a a single span slab on girders bridge located in a western suburb of Chicago, Illinois. The bridge is 20.27 m (66.5 ft) long and has an overall width of 16.00 m (52.5 ft). The beams were supported on fixed bearings at the west end and rockers at the east end. Prior to the field testing of the bridge it was modeled using a commercial finite element program (ANSYS) in order to extract the modal properties and for comparison with the experimental results. The bridge remained open to traffic during the tests and therefore the accelerometers were mounted on the sidewalks. Eight optical fiber accelerometers were serially multiplexed 4 per line for the opposing sides of the bridge across the traffic lanes as shown in Fig.17. This configuration only required two channels of data acquisition and two optical fiber lead lines for the eight accelerometers. Sensor configuration allowed for the acquisition of the first bending and first torsional mode shapes of the bridge. Eight PCB piezoelectric accelerometers with the sensitivity of 1000 mv/g were also employed for comparison with the fiber optic accelerometers. Talebinejad, et al (2009) analysis of data indicated that the conventional and the fiber optic accelerometers compared well with errors of less than one percent. However, results from their preliminary numerical model did not fare well with the accelerometer data.

CONCLUSIONS

A brief summary of discrete optical fiber sensors and their applications in structural health monitoring of bridges is given in this article. Basic principles of FBG sensors and formulations leading to their calibrations are described. In general, FBG provide flexibility for design of sensors with customized sensing capabilities beyond the limitations of the conventional sensors. The geometric flexibility of these sensors renders them suitable for infrastructure applications. Example applications that are provided in the present article include monitoring of the masonry vaults of the Brooklyn Bridge, and cable stays in LingottoLingotto Bridge. Development and testing of a fiber optic FBG accelerometer was also described, including their applications in testing of a bridge in Illinois. Irrespective of the sensor, engineering judgment and knowledge about structural behavior are prerequisites to every structural monitoring activity.

REFERENCES

Ansari, F. (2007) “Practical Implementation of Optical Fiber Sensors in Civil Structural Health Monitoring," Journal of Intelligent Material Systems and Structures, Vol. 18, No. 8, 2007, pp. 879-889.

Ansari, F., De Stefano, A., and Giacosa, L.M. (2008)," Fiber optic sensors application on the SHM of a pedestrian cable-stayed bridge in Italy," in the Proceedings of SMSST'07, World Forum on Smart Materials and Smart Structures Technology (SMSST'07), Eds. Tomizuka, et al, CRC Press

Bao XY; Huang C; Zeng XD, Arcand, A., and Sullivan, P. (2002),"Simultaneous strain and temperature monitoring of the composite cure with a Brillouin-scattering-based distributed sensor," Optical Engineering, Vol. 41, No. 7, PP. 1496-1501

Berkoff, T.A., Kersey, A.D. (1996)," Experimental demonstration of a fiber Bragg grating accelerometer," IEEE Photonics Technology Letters, Vol. 8, No. 12, PP. 1677-1679

Glisic, B. (2011), "Influence of the gauge length on the accuracy of long-gauge sensors employed in monitoring of prismatic beams," Measurement Science andTechnology, Vol. 22, No. 3, DOI: 10.1088/0957-0233/22/3/035206

Glisic,B., Inaudi, D. (2010),"Distributed Fiber-Optic Sensing and Integrity Monitoring," Transportation Research Record, No. 2150 PP. 96-102

Gu, X., Chen,Z., and Ansari, F. (2000), " Embedded Fiber Optic Crack Sensor for Reinforced Concrete Structures," ACI Structural Journal, V. 97, No. 3, pp. 468-476.

Measures, R. (200), "Structural Monitoring with Fiber Optic Technology,"Academic Press, London, UK. 716 pages

Peng, F., Yang, J., Li, X., Yuan, Y., Bing, W., Ai, Z., and Yuan, L. (2011),"In-fiber integrated accelerometer," Optics Letters, Vol. 36, No. 11, pp. 2056-2058

Shi, C., Zhu, T., Rao, Y., Ming, D. (2011)" Fiber Optic Accelerometer Based on Long Period Fiber Grating Induced By CO Laser Pulses," Microwave and Optical Technology Letters, Vol. 53, No.4, pp. 841-845

Talebinejad, I., Fischer, C., Ansari, F. (2011)," A hybrid approach for safety assessment of the double span masonry vaults of the Brooklyn Bridge," Journal of Civil Structural Health Monitoring,Vol.1, No.1, pp. 3-15

Talebinejad, I; Fischer, C; Ansari, F,(2009) "Serially Multiplexed FBG Accelerometer for Structural Health Monitoring of Bridges," Journal of Smart Structures and Systems, Vol.5, No. 4, 2009, pp 345-355

Todd, M.D., Johnson, G.A., Althouse, B.A., and Vohra, S.T (1998)," Flexural beam-based fiber Bragg grating accelerometers," IEEE Photonics Technology Letters, Vol. 10, No. 1, pp. 1605-1607

Wu, Z. Zhang, H. and Yang C. (2010),"Development and Performance Evaluation of Non-slippage Optical Fiber as Brillouin Scattering-based Distributed Sensors, International Journal of Health Monitoring, Vol. 9, No. 5, PP. 413-431

Yuan, L., and Ansari, F. (1997)" White Light Interferometric Fiber Optic Distributed Strain Sensing system," Sensors and Actuators, Part A, Physical, Vol. 63, No. 3, pp. 177-84

Zhao, Y., and Ansari, F. (2002)"Embedded fiber optic sensor for characterization of interface strains in FRP composite," Sensors and Actuators A: Physical, Vol. 100, No. 2-3, PP. 247-251

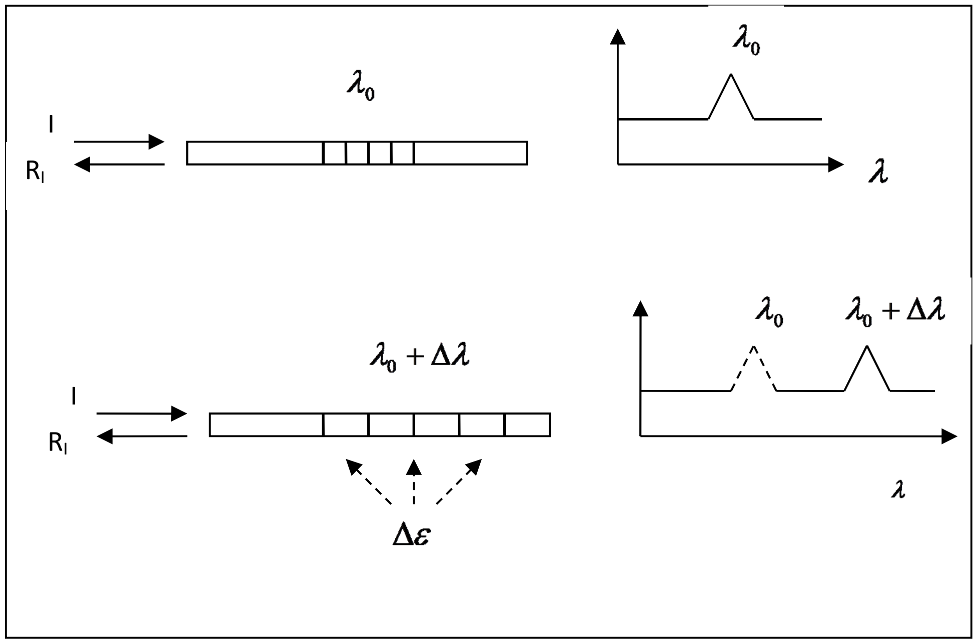

Figure 1 – Strain induced wavelength shift in FBG sensors.

Figure 2 – Masonry arch approach structures on the Manhattan side of the Brooklyn Bridge.

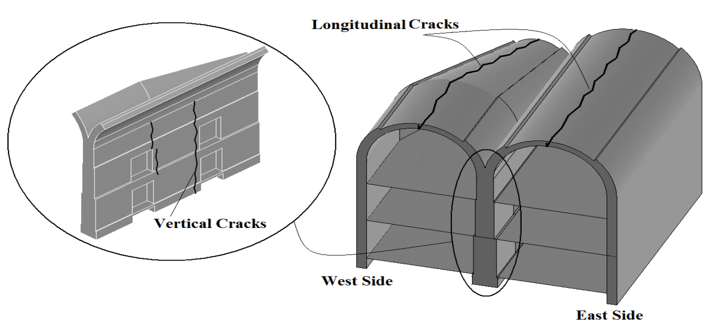

Figure 3 – Cracks in the masonry vaults and the support walls of the approach structure.

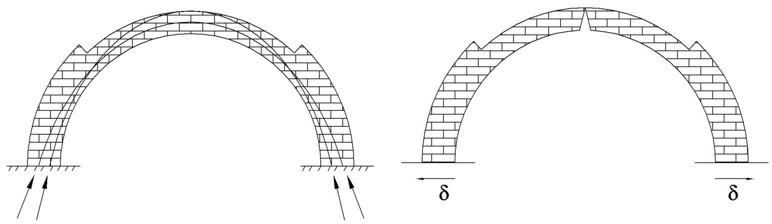

Figure 4 – Failure mechanism of the vaults.

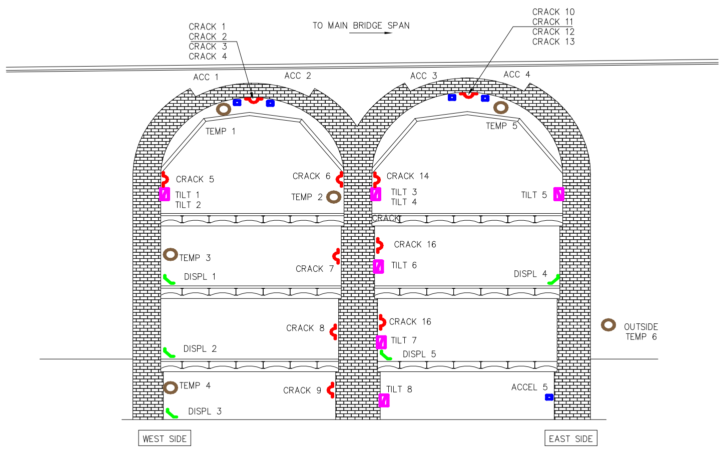

Figure 5 – Sensor layout for the double spam masonry vaults.

Figure 6 –Typical crack sensor at the crown crack and tiltmeter at the center wall

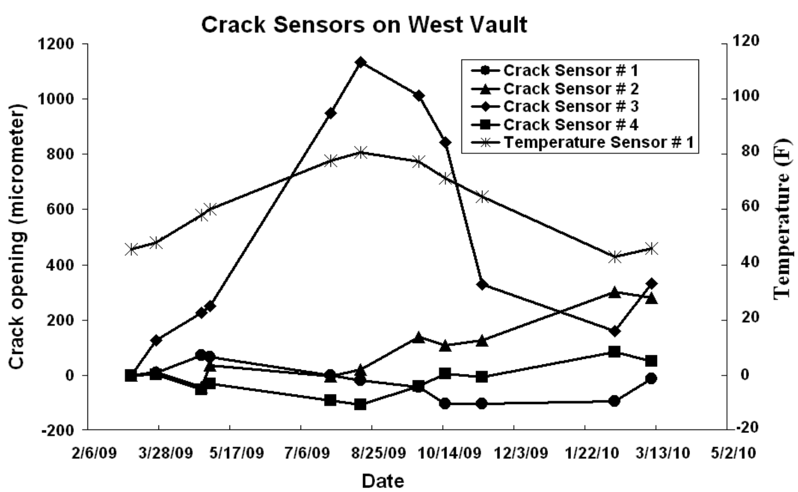

Figure 7 – Correlation of crack sensor and temperature data on the west vault over a 12 months period.

Figure 8 – LingottoLingotto Pedestrian bridge.

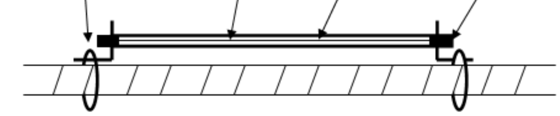

Figure 9 – FBG Cable Sensor.

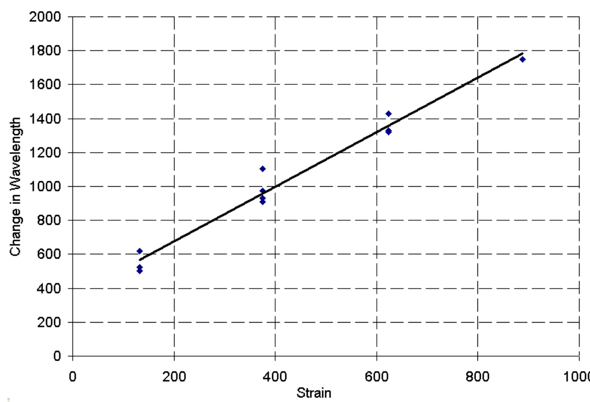

Figure 10 – Typical cable sensor calibration data.